ISSN 1674-1056
http://cpb.iphy.ac.cn
http://iopscience.iop.org/cpb
中国物理 B
Chinese Physics
中国物理 Chinese Physics B

Segregation behavior and embrittling effect of lanthanide La, Ce, Pr, and Nd at Σ3(111) tilt symmetric grain boundary in α-Fe

Jinli Cao(曹金利)[1,2], Wen Yang(杨文)[1], Xinfu He(贺新福)[1]
Citation: Chin. Phys. B . 2019, 28(12): 126802 . **doi:** 10.1088/1674-1056/ab5277
Journal homepage: http://cpb.iphy.ac.cn; http://iopscience.iop.org/cpb

What follows is a list of articles you may be interested in

Band engineering of B_2H_2 nanoribbons

Bao Lei(雷宝), Yu-Yang Zhang(张余洋), Shi-Xuan Du(杜世萱)
Chin. Phys. B . 2019, 28(4): 046803 . **doi:** 10.1088/1674-1056/28/4/046803

Adsorption and diffusion of F_2 molecules on pristine graphene

Yong Yang(杨勇), Fu-Chi Liu(刘富池), Yoshiyuki Kawazoe(川添良幸)
Chin. Phys. B . 2018, 27(10): 106801 . **doi:** 10.1088/1674-1056/27/10/106801

Effects of the $Be_{22}W$ phase formation on hydrogen retention and blistering in mixed Be/W systems

Jin-Li Cao(曹金利), Bing-Ling He(赫丙龄), Wei Xiao(肖伟), Li-Gen Wang(王立根)
Chin. Phys. B . 2017, 26(7): 076801 . **doi:** 10.1088/1674-1056/26/7/076801

First-principles study of He trapping in η-Fe_2C

Bing-Ling He(赫丙玲), Jin-Long Wang(王金龙), Zhi-Xue Tian(田之雪), Li-Juan Jiang(蒋利娟), Wei Song(宋薇), Bin Wang(王斌)
Chin. Phys. B . 2016, 25(11): 116801 . **doi:** 10.1088/1674-1056/25/11/116801

Adsorption of glycine on diamond (001): Role of bond angle ofcarbon atoms

Li Lin, Xu Jing, Xu Li-Fang, Lian Chao-Sheng, Li Jun-Jie, Wang Jian-Tao, Gu Chang-Zhi
Chin. Phys. B . 2015, 24(5): 056803 . **doi:** 10.1088/1674-1056/24/5/056803

Segregation behavior and embrittling effect of lanthanide La, Ce, Pr, and Nd at Σ3(111) tilt symmetric grain boundary in α-Fe*

Jinli Cao(曹金利)[1,2], Wen Yang(杨文)[1], and Xinfu He(贺新福)[1,†]

[1] *Reactor Engineering Technology Research Division, China Institute of Atomic Energy, Beijing* 102413, *China*
[2] *School of Materials Science and Engineering, University of Science and Technology Beijing, Beijing* 100083, *China*

(Received 27 September 2019; revised manuscript received 23 October 2019; published online 15 November 2019)

The migration of lanthanide fission products to cladding materials is recognized as one of the key causes of fuel–cladding chemical interaction (FCCI) in metallic fuels during operation. We have performed first-principles density functional theory calculations to investigate the segregation behavior of lanthanide fission products (La, Ce, Pr, and Nd) and their effects on the intergranular embrittlement at Σ3(111) tilt symmetric grain boundary (GB) in α-Fe. It is found that La and Ce atoms tend to reside at the first layer near the GB with segregation energies of −2.55 eV and −1.60 eV, respectively, while Pr and Nd atoms prefer to the core mirror plane of the GB with respective segregation energies of −1.41 eV and −1.50 eV. Our calculations also show that La, Ce, Pr, and Nd atoms all act as strong embrittlers with positive strengthening energies of 2.05 eV, 1.52 eV, 1.50 eV, and 1.64 eV, respectively, when located at their most stable sites. The embrittlement capability of four lanthanide elements can be determined by the atomic size and their magnetism characters. The present calculations are helpful for understanding the behavior of fission products La, Ce, Pr, and Nd in α-Fe.

Keywords: first-principles, fuel–cladding chemical interaction (FCCI), fission products, grain boundary segregation

PACS: 68.55.A–, 71.15.Mb, 71.15.Nc **DOI:** 10.1088/1674-1056/ab5277

1. Introduction

In the generation IV international forum, the metallic fuels for the sodium-cooled fast breeder reactor, which have been studied for more than five decades with the documented performances, were brought under renewed focus.[1] The metallic fuel pin is mainly comprised of rod-shaped fuel alloy made of U–Zr or U–Pu–Zr, HT-9 steel cladding, and the fuel-to-clad gap filled with liquid sodium.[2] They have been used in the experimental breeder reactor II (EBR-II) and qualified up to a specific burnup of 10 at.%.[3] One of the major reasons for the limitation of higher burnup is fuel–cladding chemical interactions (FCCI), which occur at the fuel and cladding interface during irradiation.[2,4–7]

FCCI is complex, including fuel–cladding interaction (e.g., U–Fe) and the interactions among fission products containing a significant mount of lanthanides (Ln) and cladding (e.g., Ln–Fe). Among them, the greatest concern of FCCI is the lanthanide–cladding interaction, as lanthanides are observed to migrate fast in a fuel and diffuse rapidly into cladding (50–150 μm),[8] yielding intermetallic precipitation, phase changes, and melting.[9–11] The lanthanide interaction with clad affects the mechanical integrity of the cladding, and is deemed a long-term, high-burnup cause of the cladding failures. Actually, fission product segregation to the grain boundary (GB) is a prerequisite for the formation of a brittle intermetallic phase. The segregation behavior could produce a significant effect on the GB cohesion, therefore limiting the ductility of the metallic alloys. Thus, the segregation of fission products and their effects on GB in the cladding is of concern, and a fundamental knowledge of these processes is needed.

Impurities and alloy elements are generally aggregated at GB, which substantially affects the mechanical properties, primary ductility, fracture toughness, and strength of metallic materials. Extensive experimental and theoretical researches have been performed on their influence on GB cohesion. For instance, interstitial boron and substitutional Mo can enhance the GB strength in Fe alloys,[12,13] while H impurities weaken GB, which is one of the mechanisms of hydrogen embrittlement.[14] On the other hand, based on the Rice–Wang model,[15] first-principles density functional theory (DFT) calculations of intergranular cohesion in the presence of segregated impurities in Fe were pioneered by Krasko and Olson, followed by extensive calculations by Freeman, Olson, and co-workers.[16–18] They employed the full potential linearized augmented-plane-wave (FPLAPW) method to study several different impurities and alloying elements at Σ3(111) symmetrical tilt GB in Fe.[18] More recently, the projector augmented wave (PAW) approach was used to study the effects of impurities on the GB. To our knowledge, there are few *ab initio* calculations for lanthanides segregation and intergranular cohesion in Fe.

The reports of post irradiation examination (PIE) data

*Project supported by the National Natural Science Foundation of China (Grant No. U1867217), the National Science and Technology Major Project of the Ministry of Science and Technology of China (Grant No. 2019ZX06004009), and the China National Nuclear Corporation Centralized Research and Development Project (Grant No. FY18000120).

†Corresponding author. E-mail: xinfuhe@gmail.com

© 2019 Chinese Physical Society and IOP Publishing Ltd

of metallic fuels (U–Zr and U–Pu–Zr) irradiated in EBR-II reactor suggested that the major lanthanides diffusing into cladding were La, Ce, Pr, and Nd.[8,19] Symmetry Σ3(111) [110] GB is a typical high-angle GB with remarkable excess volume for body-centered cubic (bcc) iron. In this work, combining first-principles calculations and the Rice–Wang model, the preferential site, segregation energy, and embrittlement capability of the four lanthanides at the Σ3(111) [110] GB in α-Fe will be investigated. We organize the remainder of the paper as follows. In Section 2, the computational methods and models are described. Section 3 presents and discusses our calculated results of the behavior of the lanthanides segregation and intergranular cohesion in α-Fe. We analyze the relaxed atomic structures of lanthanide elements at Σ3(111) GB and the corresponding excess volume to understand the physical origin of segregation and embrittling behavior of these impurities. Finally, a short summary is given in Section 4.

2. Computational methods and models

Our first-principles DFT calculations were performed using the Vienna *ab initio* simulation package (VASP).[20–22] The interaction between valence electron and nuclei was obtained using the projector augmented wave (PAW) method.[23,24] The exchange and correlation terms in DFT method were treated with generalized gradient approximation (GGA) in the Perdew–Burke–Ernzerhof (PBE) form.[25] A conjugate gradient algorithm was used to relax the atomic positions to a local minimum in the total energy landscape. The cut-off energy for the plane wave basic set was 350 eV. For each system, geometry optimization could continue until the total energy of this system was converged to less than 10^{-4} eV. A $7\times4\times1$ k-mesh in Monkhorst–Pack scheme replaced the integration over Brillouin zone in the following simulation.[26]

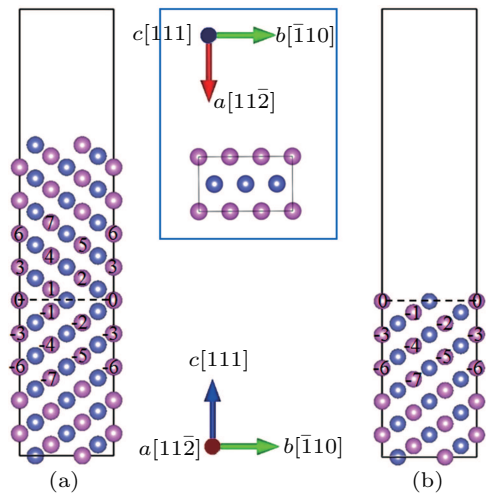


Fig. 1. Computational models: (a) Σ3(111)[1$\bar{1}$0] tilt GB with 29 layers and (b) the Fe (111) free surface (FS) with 15 layers. The violet and blue spheres represent atoms on the (11$\bar{2}$) and (22$\bar{4}$) planes, respectively. The numbers here are used to denote different positions near the GB and surface.

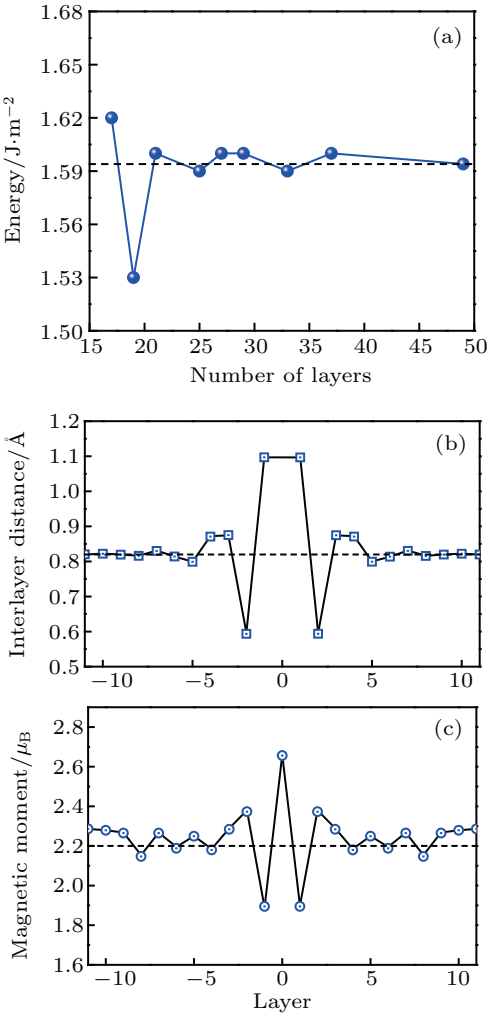


Fig. 2. (a) The GB formation energy for cells containing different numbers of atomic layers from 17 to 49. (b) Relaxed interlayer distance in the Fe grains near the boundary. The (111) interlayer distance in the bulk truncated Fe is 0.82 Å. (c) Magnetic moment on Fe atoms at various layers in the vicinity of the GB (cf. Fig. 1). Horizontal dash line marks the magnetic moment of the bulk Fe.

We selected the Σ3(111)[1$\bar{1}$0] tilt GB as a prototype low-energy symmetric twin boundary in bcc Fe, and modeled the GB using a supercell illustrated in Fig. 1(a). One supercell was composed of two identical grains (each contains 15 atomic layers with one in common), which formed a symmetric tilt GB in between. The two-dimensional lattice constant for the stress-free systems was chosen to be the bulk value of bcc Fe, 2.83 Å, which was also reproduced in our GGA-PBE computation. Since we have used a periodic boundary condition, we separated the neighboring slabs in [111] direction by a vacuum region of at least 10 Å to minimize the interaction between the slabs. Test calculations on GB energy for cells containing different numbers of atomic layers from 17 to 49 were carried out, and the results are shown in Fig. 2(a). It can be seen that the GB formation energy converges to 1.59–1.60 J/m^2 when the layer of GB slabs is larger than 21. On the other hand, we also display the calculated interlayer distance and magnetic moment on Fe atoms near the GB in Figs. 2(b) and 2(c), respectively. It is clearly seen that the oscillatory is very large

near the GB center, and then decays toward the bulk layers (from site 6). In comparison to the ideal grains, the relaxations cause an increase of 0.24 Å in the excess volume per unit area, which offers a larger space available for the impurity element. In Fig. 2(c), the moments exhibit a damped oscillatory convergence toward 2.20 μ_B for the deeper grain layers. These results show that the 29-layer slab is thick enough to mimic a bulk-like environment in the middle of each grain.

In order to assess the tendency of the fission product to segregate to the GB from the bulk environment, the segregation energy of one X atom (X = La, Ce, Pr, and Nd) at GB is defined by

$$E_{\text{seg}} = E^X_{\text{GB}} - E^X_{\text{bulk}}, \tag{1}$$

where E^X_{GB} and E^X_{bulk} are the total energies of the system with X atom near the GB and in the bulk (site 7) far away from the GB, respectively. As shown in Figs. 2(b) and 2(c), site 7 can be chosen as the substitutional site with a bulk-like atomic environment. The negative means that Ln X can segregate at the GB.

Since lanthanides La, Ce, Pr, and Nd are rare earth elements with strongly localized f electrons, it should be careful for their first-principles calculations. In transitional metal oxides or cerium oxides, Hubbard U correction to the standard DFT calculation works well for adjusting the band gap by taking into account of the orbital dependence of the intra-atomic Coulomb interaction.[27] In fact, the empirical Hubbard U correction is controversial for the first-principles calculations. In the recent work, Chen *et al.* studied the electronic and optical properties of rare-earth-doped VO_2 nanoparticles,[28] they did not apply Hubbard U correction on lanthanides but on vanadium. Furthermore, Hao proved that the on-site Coulomb interaction has little effect on the description of Ce in iron solid solutions.[29] In view of this fact, we have selected Nd with most 4f electrons to examine the effect of the on-site Coulomb interaction on the segregation energy of Nd at GB in iron in GGA $+U$ calculations. The results are listed in Table 1, and suggest that the on-site Coulomb interaction has only a marginal effect on the interaction between Nd and GB (0.02–0.03 eV). Therefore, we conclude that GGA can deal with the Ln–Fe alloy system well enough and we will proceed with our investigations using only GGA treatment in the work.

Table 1. Dependence of the segregation energy of Nd at the GB (in eV), defined by Eq. (1) in bcc Fe on Hubbard U, the effective on-site Coulomb interaction (in eV).

E_{seg}	Site 0	Site 1	Site 2	Site 3	Site 4
$U = 0$	–1.50	–1.48	–1.48	–1.22	–0.13
$U = 4$	–1.53	–1.51	–1.49	–1.25	–0.15

3. Results and discussion

3.1. Segregation of lanthanides near GB

Lanthanides, with large atomic size, could prefer to occupy a substitutional site rather than an interstitial site. We could examine the segregation behaviors by putting fission product X atom at five different substitutional sites near the GB, sites 0–4 in Fig. 1. The calculated segregation energies for La, Ce, Pr, and Nd atoms toward to the GB are summarized in Table 2. Figure 3 plots the atomic configurations of different fission products favorably segregated to the GB after relaxations. Apparently, Ln atoms all tend to segregate to $\Sigma3(111)[1\bar{1}0]$ tilt GB from bulk environment with a large driving energetic force from 1.41 eV to 2.55 eV. For La and Ce, they tend to locate at the first layer (site 1) of the GB with segregation energies of −2.55 eV and −1.60 eV, while Pr and Nd atoms prefer the core mirror plane (site 0) near the GB with lower segregation energies of −1.41 eV and −1.50 eV. In the cases of La and Ce, we can see that the upper and lower atoms of the GB all slip in the opposite directions, and the atoms in the mirror plane of GB deviate from the original positions in Figs. 3(a) and 3(b). The large excess volume offers a larger space available for the Ln elements. Moreover, their slipping and deviations result in the larger driving force for lanthanides segregation to the GB.

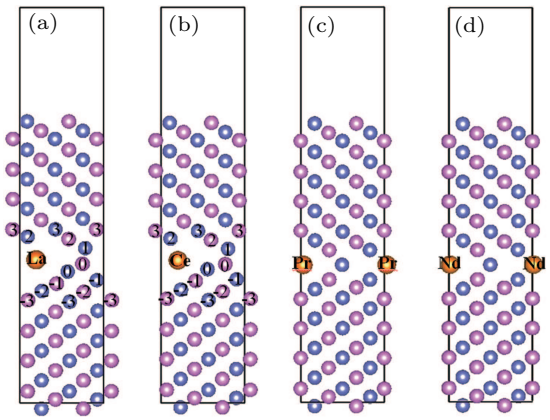


Fig. 3. Atomic configurations of fission products (a) La, (b) Ce, (c) Pr, and (d) Nd favorably segregated to $\Sigma3(111)[1\bar{1}0]$ tilt GB after relaxations, respectively. For La and Ce, the initial positions are site 1, while site 0 for Pr and Nd. We label the positions by the numbers near the GBs for La and Ce.

Table 2. Calculated segregation energy (in eV) of a La, Ce, Pr, or Nd atom at substitutional sites 0–4 near the GB.

E_{seg}	Site 0	Site 1	Site 2	Site 3	Site 4
La	–1.93	–2.55	–2.28	–1.52	–0.07
Ce	–1.51	–1.60	–1.32	–1.22	–0.10
Pr	–1.41	–0.76	–1.40	–1.14	–0.15
Nd	–1.50	–1.48	–1.48	–1.22	–0.13

As we know, we can estimate the occupation probability of the impurity near the GB using the McLean's equation[30]

$$C_{\text{GB}} = \frac{C_{\text{bulk}} \exp(-E_{\text{seg}}/k_{\text{B}}T)}{1 + C_{\text{bulk}} \exp(-E_{\text{seg}}/k_{\text{B}}T)}, \tag{2}$$

where E_{seg} is the segregation energy of the impurity near the GB, C_{bulk} is the concentration of the impurities in a bulk material, k_B is the Boltzmann's constant, and T is the aging temperature. In the sodium-cooled fast breeder reactor, the operating temperature span of cladding is from 600 K to 900 K. In our estimation, we consider three typical temperatures, including room temperature 300 K, lower operating temperature 600 K, and the peak temperature 900 K to discuss the segregation behavior near the GB. The production rate of fission product Ln in the fuel is only 2–10 appm (atomic parts per million) per year in fast reactors. However, they diffuse down the temperature gradient and are found in relatively high concentration at the fuel/cladding surface. In MOOSE/BISON modelling of Ln in fuel,[31] the Ln source is even supposed as 10^4 appm/year. We thus investigate three impurity concentrations in the bulk, 1 appm, 10^2 appm, 10^4 appm in our work.

Based on the McLean's equation, we present the occupation probability at three temperatures for various impurity concentrations in the bulk in Fig. 4. Apparently, more impurity atoms could be located at the GB for the larger segregation energy, lower temperature, and higher concentration in the bulk. Table 2 suggests that the Ln atoms have a strong tendency to segregate to the GB with segregation energies from -1.41 eV to -2.55 eV. From Fig. 4, we can see that their occupation probabilities in GB (0) or GB (1) are close to one for a large temperature span of 300–900 K. Therefore, our discussion on segregation of highly concentrated Ln at low temperature is meaningful, and most fission products Ln could thermodynamically segregate to the GB at the operating environment.

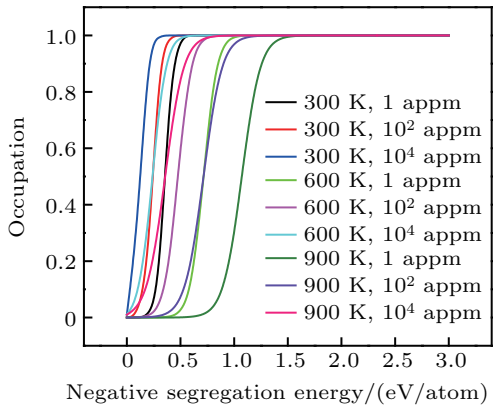


Fig. 4. The calculated occupation probability of Ln atoms near the GB sites as a function of the segregation energy at different temperatures and bulk concentrations based on the Mc-Leans' equation.

3.2. Effects of lanthanide on GB cohesion

In order to discuss the effects of fission products La, Ce, Pr, and Nd atoms on GB cohesion, it is convenient to investigate the strengthening energy based on the thermodynamic approach of Rice and Wang.[15] Within the first-principles calculation, it can be defined as the difference between the binding energy of an impurity to the GB and that to the FS slab, $\Delta E = \Delta E_b^X - \Delta E_s^X$, where ΔE_b^X and ΔE_s^X are the binding energies of an impurity to the GB and to the FS, respectively. Simultaneously subtracting the total energy of an isolated impurity, the strengthening energy can be written as

$$\Delta E = E(X/\mathrm{GB}) - E(\mathrm{GB}) - [E(X/\mathrm{FS}) - E(\mathrm{FS})], \quad (3)$$

where $E(X/\mathrm{GB})$, $E(\mathrm{GB})$, $E(X/\mathrm{FS})$, and $E(\mathrm{FS})$ represent the total energies of the X segregated GB, clean GB, X adsorbed FS, and clean FS slabs, respectively. A positive (negative) value suggests that an impurity is an embrittler (strengthener) at the GB.

The fission products have a strong driving force to segregate to the GB with a range of 4 layers, not only for mirror plane site 0, but for sites 1, 2, and 3 in Table 2. According to formula (3), the calculated strengthening energies of La, Ce, Pr, and Nd at different substitutional sites near the GB are displayed in Fig. 5. Located at the most stable sites, La, Ce, Pr, and Nd atoms all act as strong embrittlers with positive strengthening energies of 2.05 eV, 1.52 eV, 1.50 eV, and 1.64 eV, respectively. As for the other sites, due to the lower binding energy with GB, they generally show stronger embrittling effects, even with a strengthening energy of more than 3.00 eV for La at site 3. In Fig. 5, we can obtain that the embrittlement capability of La element is much stronger than that of Ce, Pr, and Nd. The capability of Nd is slightly stronger than that of Ce and Pr for most stable sites near the GB. Therefore, to sum up, the embrittlement ability of four lanthanide elements is in the order of La > Nd > Ce ≈ Pr.

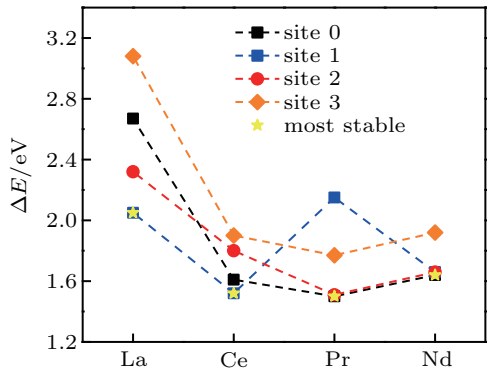


Fig. 5. The calculated strengthening energies of different Ln atoms located at different sites near $\Sigma3(111)[1\bar{1}0]$ tilt GB in α-Fe. The yellow stars present the embrittlement energies of Ln atoms at their most stable sites.

The embrittlement behaviors of four lanthanide elements above can be attributed to the atomic size of Ln atoms and their magnetism characters. It has been shown that the relative embrittling or cohesion enhancing behavior of segregated impurity atoms is mainly determined by the atomic size and their bonding properties.[18] As we know, the atomic sizes of lanthanide elements gradually decrease as the atomic number increases. At first, the excess volume change caused by Ln absorbed to the GB can be generally an evaluation of atomic

size. In Fig. 6, we depict their excess volume change after the GB relaxation, and the calculated embrittlement energies of Ln atoms at their most stable sites for direct view. Apparently, the trend of embrittlement energies is closely related to the excess volume change. Due to the largest atomic size, La segregation to the GB could lead to the maximum excess volume change, 0.86 Å. It acts as the strongest embrittler, followed by Ce and Pr. Among these elements, Nd is an exception, because it has a slightly larger embrittlement energy than Ce and Pr and the minimum excess volume change. We can attribute these to its special large antiferromagnetic moment, $-3.14\ \mu_B$. For La, Ce, and Pr at the GB, their local magnetic moments are $-0.14\ \mu_B$, $-0.40\ \mu_B$, and $-1.77\ \mu_B$, respectively. The magnetic interactions have been proved to be strongly coupled with the binding or repulsive characteristic of the defects at the GBs.[32,33]

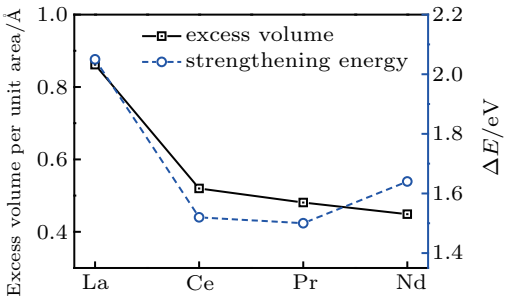


Fig. 6. Change in the excess volume per unit area of the Fe GB caused by Ln impurity placed in the most stable sites and calculated embrittlement energies of Ln atoms at their most stable sites.

4. Conclusion

Using first-principles density calculations, we have investigated the segregation energy of Ln fission products (La, Ce, Pr, and Nd) near Σ3(111) tilt symmetric GB and their effects on the intergranular embrittlement in α-Fe. Firstly, we determined the segregation energies of La, Ce, Pr, and Nd at different substitutional sites near the GB. The results show that they all tend to segregate to Σ3(111)[1$\bar{1}$0] tilt GB from bulk environment with a large energetic driving force. For La and Ce, they tend to locate at the first layer (site 1) near the GB with segregation energies of -2.55 eV and -1.60 eV, while Pr and Nd atoms prefer to occupy the core mirror plane (site 0) of the GB with lower segregation energies of -1.41 eV and -1.50 eV. Atomic configuration analysis shows that the absorption of La and Ce to the GB could cause the slipping of the upper and lower atoms of the GB and the deviation of atoms in the mirror plane. Based on the McLean's equation, we thermodynamically evaluated their occupation probabilities near the GB. The strong driving forces to segregate to the GB make the fission product highly concentrate at the GB at the operating environment. Besides, based on Rice and Wang model, we have obtained that La, Ce, Pr, and Nd atoms are all strong embrittlers with strengthening energies of 2.05 eV, 1.52 eV, 1.50 eV, and 1.64 eV, respectively. The embrittlement capability of these four lanthanide elements can be determined by the factors of their atomic size and magnetism.

Acknowledgement

We appreciate useful discussions with Wei Xiao and Yankun Dou.

References

[1] Delage F, CarmackbC J, Leec B, Mizunod T, Pelletiera M and Somerse J 2013 *J. Nucl. Mater.* **441** 515
[2] Carmack W J 2009 *J. Nucl. Mater.* **392** 139
[3] Hofman G L, Walters L C and Bauer T H 1997 *Prog. Nucl. Energ.* **31** 83
[4] Cohen A B, Tsai H and Neimark L A 1993 *J. Nucl. Mater.* **204** 244
[5] Xie Y, Zhang J S, Benson M T, King J A and Mariani R D 2019 *J. Nucl. Mater.* **513** 175
[6] Xie Y, Benson M T, King J A, Mariani R D and Zhang J S 2018 *J. Nucl. Mater.* **498** 332
[7] Ogata T, Kurata M, Nakamura K, Itoh A and Akabori M 1997 *J. Nucl. Mater.* **250** 171
[8] Matthews C, Unal C, Galloway J, Dennis D K J and Hayes S L 2017 *Nucl. Technol.* **198** 231
[9] Kim J H 2014 *Met. Mater. Int.* **20** 819
[10] Kim J H 2012 *J. Rare Earths* **30** 599
[11] Chuang Y C, Wu C H and Shao Z B 1987 *J. Less Common Met.* **136** 147
[12] Liu C M, Nagoya T, Abiko K and Kimura H 1992 *Metall. Trans. A* **23** 263
[13] Lee D Y, Barrera E V, Stark J P and Marcus H L 1984 *Metall. Trans. A* **15** 1415
[14] Kimura A and Kimura H 1986 *Mater. Sci. Eng.* **77** 75
[15] Rice J R and Wang J S 1989 *Mater. Sci. Eng. A* **107** 23
[16] Krasko G L and Olson G 1991 *Solid State Commun.* **79** 113
[17] Wu R, Freeman A J and Olson G B 1994 *Science* **265** 376
[18] Geng W T, Freeman A J and Olson G B 2001 *Phys. Rev. B* **63** 165415
[19] Mariani R D 2011 *J. Nucl. Mater.* **419** 263
[20] Kresse G and Furthmüller J 1996 *Phys. Rev. B* **54** 11169
[21] Kresse G and Hafner J 1993 *Phys. Rev. B* **47** 558
[22] Kresse G and Furthmüller J 1996 *Comp. Mater. Sci.* **6** 15
[23] Kresse G and Joubert D 1999 *Phys. Rev. B* **59** 1758
[24] Blöchl P E 1994 *Phys. Rev. B* **50** 17953
[25] Perdew J P, Burke K and Ernzerhof M 1996 *Phys. Rev. Lett.* **77** 3865
[26] Monkhorst H J and Pack J D 1976 *Phys. Rev. B* **13** 5188
[27] Zhang L F 2018 *Inorg. Chem.* **57** 12690
[28] Chen L L 2019 *Com. Mater. Sci.* **161** 415
[29] Hao W and Geng W T 2010 *Nucl. Instru. Methods Phys. Res. B* **280** 22
[30] McLean Donald 1957 *Grain boundaries in metals* (Oxford: Oxford University Press) p. 347
[31] Zhang J S 2017 *Studies of Lanthanide transport in metallic fuel*, Chapter **8**
[32] Tian Z X, Yan J X, Xiao W and Geng W T 2009 *Phys. Rev. B* **79** 144114
[33] Wachowicz E, Ossowski T and Kiejna A 2010 *Phys. Rev. B* **81** 094104